

Precise Onboard Aircraft Cabin Localization using UWB and ML

Fabien Geyer and Dominic Schupke
Airbus Central R&T, Munich, Germany

Abstract—Precise indoor positioning systems (IPSs) are key to perform a set of tasks more efficiently during aircraft production, operation and maintenance. For instance, IPSs can overcome the tedious task of configuring (wireless) sensor nodes in an aircraft cabin. Although various solutions based on technologies of established consumer goods, e.g., Bluetooth or WiFi, have been proposed and tested, the published accuracy results fail to make these technologies relevant for many use cases. This stems from the challenging environments for positioning, especially in aircraft cabins, which is mainly due to the geometries, many obstacles, and highly reflective materials. To address these issues, we propose to evaluate in this work an Ultra-Wideband (UWB)-based IPS via a measurement campaign performed in a real aircraft cabin. We first illustrate the difficulties that an IPS faces in an aircraft cabin, by studying the signal propagation effects which were measured. We then investigate the ranging and localization accuracies of our IPS. Finally, we also introduce various methods based on machine learning (ML) for correcting the ranging measurements and demonstrate that we are able to localize a node with respect to an aircraft seat with a measured likelihood of 97 %.

I. INTRODUCTION

Indoor positioning systems (IPSs) are a necessary step towards automation across various industries. Comprehensive research has been performed in indoor positioning using different technologies such as Bluetooth, WiFi, Ultra-Wideband (UWB), each with different algorithms such as trilateration, triangulation, or fingerprinting [1, 2]. While promising centimeter-level accuracy solutions are available when line-of-sight (LOS) paths are available, it is hard to maintain that accuracy in harsh indoor conditions with human blockage, obstacles or reflective materials. One of the challenging closed areas is the cabin of an aircraft, where various obstacles are present such as seats, humans, or luggage, making it significantly different from the residential, office, outdoor or industrial environments [3, 4]. As shown later in Section V, this leads to an environment with mostly non-line-of-sight (NLOS) conditions and with a high number of multipaths, making it generally difficult for accurate localization.

A precise IPS would enable automatic localizing of not only wireless sensors that measure, e.g., temperature or cabin air pressure once aircraft operations started, but also other tagged items such as life vests. In this way, cost and time savings are possible by avoiding largely manual configuration of sensors in assembly lines and by supporting cabin crew operations, such as item checks, before and after flights.

In order to be of broader use in an aircraft cabin scenario, the IPS should be able to distinguish between cabin seats, represented by an absolute localization error of approximately 20 cm in 2D. UWB has already been shown to be a promising candidate technology for cabin wireless communication and for such a localization requirement [5, 6, 7].

While these previous works were limited to small mockups of aircraft cabins, we extend here our evaluation of UWB to a larger scale measurement campaign performed in a full-scale cabin of an Airbus A321. Two different scenarios are evaluated, where the object to be localized is either placed near the seat or near the seat's headrest. We perform a comparison between traditional multilateration techniques and improved methods based on neural networks (NNs). We also contribute additional methods based on NN, and show how an end-to-end training approach achieves the localization accuracy.

Overall, our measurements illustrate the challenge that an aircraft cabin constitutes with respect to received signal strength indication (RSSI)-based and UWB-based IPSs. We show the influence that the cabin has on the physical properties of the radio frequency (RF) signals compared with outdoor and office environments free of obstacles. We demonstrate that our IPS is able to achieve an average localization error of 16.7 cm and a seat assignment error of 97 %, almost fulfilling our industrial requirements for all the seats in the aircraft.

This work is organized as follows: Section II presents the related work and Section III introduces the evaluated localization system and its use-cases for aircraft cabins. Section IV introduces the various methods for improving the accuracy of the IPS. Section V describes our measurement campaign and localization results. Section VI concludes this work.

II. RELATED WORK

A. UWB for localization

UWB-based localization has attracted a large body of works, mainly due to the high accuracy possible by the extremely large spectrum. Various works investigated the effects of the environment on the properties of the RF channel. Irahauten et al. [8] reported measurements and modeling of the UWB indoor wireless channel. They concluded that there is a limited temporal correlation between powers of multipath components and that acUWB is more robust against fading than conventional narrowband and wide-band systems. Ye et al. [9] quantified the effect of LOS and NLOS on ranging in real indoor and outdoor environments. They evaluated the impact of various materials and conditions on the ranging error.

Various works investigated how to account for NLOS on the ranging accuracy. Ngo et al. [10] proposed a solution based on geometric modeling of the environment. Bandiera et al. [11] proposed an approach based on machine learning (ML) to identify the environment and estimate its relevant propagation parameters. Schroeer [12] used UWB-based localization in industrial scenarios with anchors based on four transceivers. They demonstrated an average accuracy of 0.13 m.

Alternate uses of UWB-based ranging were also recently investigated by using the additional channel impulse response (CIR) data, which characterizes the RF signal propagation. Ledergerber et al. [13] proposed to evaluate CIR for angle of arrival estimation. Ledergerber and D'Andrea [14] illustrated how CIR post-processing can be used for building a multi-static radar network, demonstrating the localization of a tag-free human walking in a room. Various works also used ML for correcting localization error. Kram et al. [15] used the CIR in order to predict information about localization.

B. UWB for aircraft applications UWB based IPS (aircraft cabin)

UWB has already been investigated as a solution for on-board wireless communication in aircraft cabin. Chiu et al. [3][4] characterized the UWB RF propagation and CIR within the passenger cabin of a Boeing 737-200 aircraft. They reported the fading statistics and correlation properties of individual multipath components (MPCs). The effect of human presence was also evaluated and demonstrated how it affects the path gain. Andersen et al. [16] also investigated the impact of passengers on UWB signal absorption at different sections of a large wide-bodied aircraft mockup. They concluded that the effect of passengers was marginal for the tested configuration. Neuhold et al. [17] proposed a proof-of-concept for an UWB sensor network deployed in a mockup of a small passenger cabin of a commercial aircraft with a few passengers and measured packet loss rate. They evaluated the loss induced by a single passenger and seat row and demonstrated packet loss rates with respect to signal attenuation.

Schmidt et al. [6] showed how UWB is a particularly fitting technology to support intra-aircraft communications and investigated regulation aspects. Via a proof-of-concept implementation, they also highlighted the potential of UWB for intra-aircraft use and identify challenges ahead.

In our previous work [5], we already investigated the localization accuracy of a UWB-based localization system, but it was limited to a small section in a cabin mockup. To the best of our knowledge, this is the first work presenting such measurement campaign of UWB-based IPS onboard a real aircraft cabin. Compared also with previous works using ML for UWB-based localization, we are proposing a true end-to-end approach where the localization is directly predicted by the NN based on the raw data provided during ranging.

III. LOCALIZATION SYSTEM

We introduce in this section the IPS used for our evaluation. UWB was selected for our IPS mainly because of its high accuracy, its low latency, and its strong immunity against

multipath conditions compared with other solutions such as WiFi or Bluetooth-based solutions.

A. Use-cases

An IPS inside an aircraft cabin is highly relevant in order to assist the optimization and automation of many industrial and operational processes, from the manufacturing phase until the end of life of an aircraft.

It is expected to have hundreds to thousands of wireless sensors placed inside the aircraft monitoring the environment and devices status using sensors such as temperature, humidity, engine status, smoke detection, cabin pressure, seat, or door status [18, 19, 20]. The position of each sensor is used in order to properly correlate the measured data with the corresponding area of the aircraft. Another application is to localize and identify seats. Currently, the position of each seat and their corresponding numbers are hard-coded in a database based on the cabin configuration, dependent on each airline. However, a localization system may localize seats and automatically assign seat numbers with sensors placed around it. Various tasks have to be performed by the cabin crew before each take-off and after landing. Before aircraft take-off, the presence of safety equipment such as life vests, fire extinguishers, or first aid kits has to be checked. An IPS could automatically identify the location of items to be checked.

Finally, various works already demonstrated that the UWB technology can be made compliant with respect to regulations for aircraft and cabin communications [6, 7].

B. UWB-based ranging

Our system is based on the Qorvo EVB1000 and DWM1001 evaluation boards, a system promising centimeter-level accuracy with a measurement latency of a few milliseconds. The Qorvo platform provides an easy-to-use system for working with UWB and supports custom software running directly on the micro-controller of the evaluations boards.

Both platforms are based on the DW1000 chip, which provides the facilities for message time-stamping and precise control of message transmission times. This enables a ranging method known as two way ranging (TWR), where the time of flight (ToF) between two nodes can be measured by exchanging packets and measuring their time of arrival.

C. Platform

The system is composed of two types of nodes. Firstly, anchor nodes are placed throughout the measurement environment at known locations. Secondly, tag nodes with unknown prior localization can then be localized by measuring their distance with the anchors via the TWR process.

A simple controller/agent architecture was developed, which ensures that only a single node can send a packet at a time, preventing packet collisions. For each ranging measurement between the tag and one of the anchors, the tag reports the resulting ToF, the values of the various diagnostic registers from the DW1000, and the CIR buffer to a central computer collecting all the data. The CIR contains information about the RF signal properties of the underlying propagation paths.

After the ranging process is finished, the multilateration phase is performed in order to compute the 2D localization of the tag. The following optimization problem is solved:

$$\min_{x_T, y_T} \sum_i ((x_T - x_i)^2 + (y_T - y_i)^2 + \delta_z^2 - r_i^2)^2 \quad (1)$$

with (x_T, y_T) the coordinates of the tag which need to be computed, (x_i, y_i) the known coordinates of the anchor i , δ_z the known distance along the z axis, and r_i the distance between the tag and anchor i .

IV. LOCALIZATION IMPROVEMENTS

The accuracy of the localization and multilateration approach presented earlier is highly dependent on the accuracy of the ranges and the measurement environment. A first evaluation of the raw ranging values provided by the system showed an average absolute error of 0.6 m in our aircraft cabin.

The DW1000 chip already provides mitigation techniques to overcome multipath effects in NLOS environments [21]. Despite these, our evaluation still showed a consistent non-negligible ranging error. We propose in this section different approaches for improving the overall accuracy of the system.

A. Static offset

For this first approach, we apply a static offset to each ranging measurement:

$$\text{corrected range} = \text{range} + o_i \quad (2)$$

with o_i the parameter of the model, fitted for each anchor i in the system. This is the simplest error correction model, which can compensate for static delays for the TWR process.

B. Linear regression

An improvement of the previous model is to take into account the impact of the range on the error. We model this effect using linear regression (LR):

$$\text{corrected range} = \text{range} \cdot a_i + b_i \quad (3)$$

with a_i and b_i parameters of the model, which are fitted for each anchor i in the system.

C. Neural network

We propose in this section a NN-based approach to predict various aspects about the localization. We introduce here various extensions to our previous work [5], with additional output types and a fully end-to-end training and prediction.

Our NN architecture is illustrated in Figure 1. As input, a vector concatenating the measured ranges and CIR data of one or all the anchors is used. This vector is then processed by three fully-connected NN layers with ReLU activation. As output, the NN predicts either the ranges, the coordinates of the tag, or the seat label as presented in Table I.

In total, we trained four different versions of the NN, presented in Table I. The first two versions (NN 1A and NN range pred.) still require the multilateration step presented in Section III-C and Equation (1) in order to compute the 2D

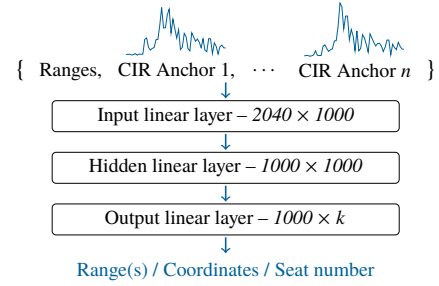


Fig. 1: Architecture of the NN and the size of the layers. The size of the last layer depends on the type of output required.

localization of the tag. The last two versions follow an end-to-end approach and directly predict the tag's position, either as 2D coordinates or as label. This means that the optimization step from Equation (1) is not required for these versions in order to compute the 2D localization of the tag.

TABLE I: Variants of the neural network used in our evaluation

Label	Inputs	Outputs	Problem
NN 1A	1 anchor	1 range	Regression
NN range pred.	All anchors	All ranges	Regression
NN coord. pred.	All anchors	Coord. of the tag	Regression
NN seat pred.	All anchors	Seat label	Classif.

V. NUMERICAL EVALUATION

We describe in this section our measurement campaign and the ranging and localization results which were measured.

A. Measurement environments

Our measurements were performed in a real cabin of an Airbus A321 fully furnished with 161 seats, specifically used for tests and measurements located at the Airbus manufacturing plant in Finkenwerder, Germany. The cabin layout is illustrated in Figure 2a. In total, 11 anchors were placed throughout the cabin according to Figure 3 using Qorvo's MDEK1001 development module. In order to assess a potential industrial installation, the anchors were placed inside the luggage compartments as close to the cabin's hull as possible.

For our ranging measurements, Qorvo's EVK1000 evaluation kit was used as the tag to be localized. All 161 seats in the cabin were measured, with two different positions: directly on the seat as illustrated on Figure 2b, or on the headrest as illustrated on Figure 2c. For each position, 10 different ranging measurements were performed, 7 of them used for training the various NNs and 3 for the evaluation presented here.

As a comparison, we also performed measurements in two additional environments: outside and in an indoor office environment, both with LOS conditions.

B. Impact of the environment on the RF signal

We first review the impact of the different measurement environments on the properties of the physical RF signal.

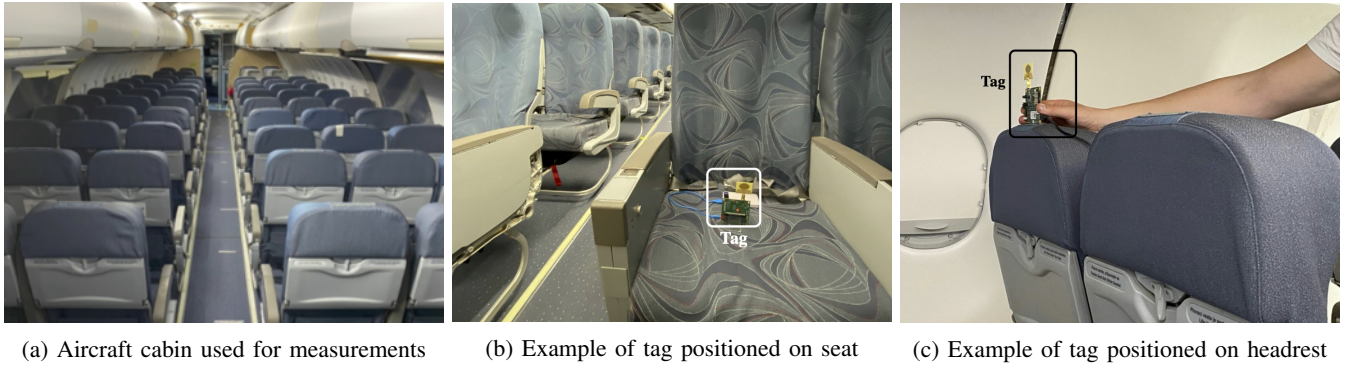


Fig. 2: Measurement environment and tag positioning

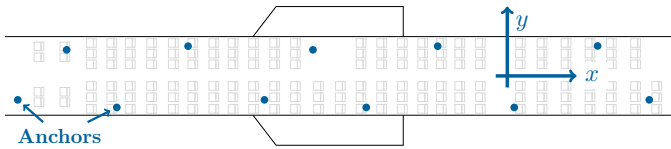


Fig. 3: A321 cabin layout and anchor placements. The position of each seat was measured during our measurement campaign.

Two samples of the CIR data are presented in Figure 4, one in the aircraft cabin, and the other in the indoor office environment, both for a distance between the nodes of approximately 10 m. While both environments exhibit multipath effects, the magnitude of this effect is much larger in the aircraft environment. We also notice a stronger fading of the RF signal in the aircraft environment.

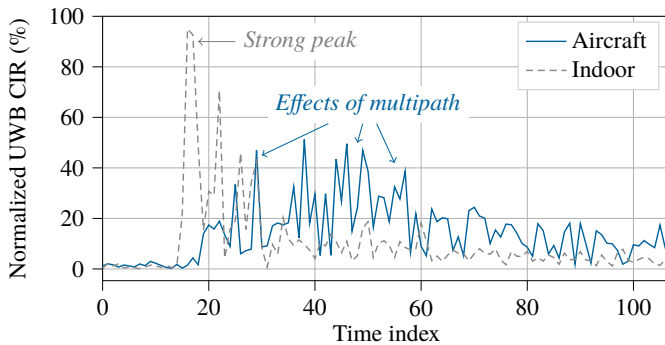


Fig. 4: Example of CIR data. The effects of multipath are clearly seen in the cabin compared to the indoor environment.

To numerically assess the fading of the RF signal, we use the first path power level as our metric. Based on Qorvo's documentation, we use the following estimation formula:

$$10 \cdot \log_{10} \left(\frac{F_1^2 + F_2^2 + F_3^2}{N^2} \right) - A \quad (4)$$

where F_i corresponds to the first path amplitude point i registers, and A a constant dependent on the radio configuration.

The impact of the ranging distance on the first path power levels are presented in Figure 5. Compared with the outdoor

and indoor environments, there is a much stronger attenuation on the received signal power in the aircraft, mainly due to the higher number of obstacles. This strong attenuation had an impact on the connectivity, since ranging between the extreme front and back of the cabin was difficult due to the power levels below the DW1000 sensitivity.

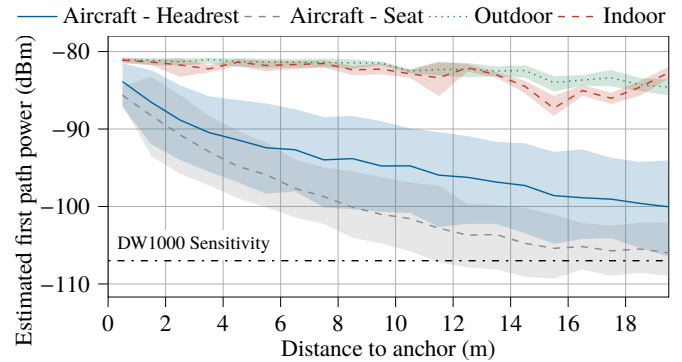


Fig. 5: Impact of distance on estimated first path power level. Areas correspond to the 25 % and 75 % percentiles.

We note also in Figure 5 a correlation between the estimated first path power and the distance to anchor. This relationship is often used in well-known localization methods such as Bluetooth-based or WiFi-based systems, which use RSSI information for distance estimation. To understand how such system would have performed in our measurement environment, we fitted a polynomial of degree 3 to the data and computed the resulting absolute ranging error of such a RSSI-based system. Results are presented in Figure 6. Compared to the non-corrected values provided by the UWB ranging system, the RSSI-based estimator provides worst results, with an average absolute error of 2.52 m. This demonstrates why RSSI-based systems are not sufficient for our use-cases and motivates our choice of a UWB-based system.

Finally, we also numerically quantify the multipath effects visible on Figure 4 with the following metric:

$$\text{multipath metric} = \frac{1}{N-1} \sum_{i=1}^N \left(1 - \frac{\text{CIR}_i}{\max_k \text{CIR}_k} \right) \quad (5)$$

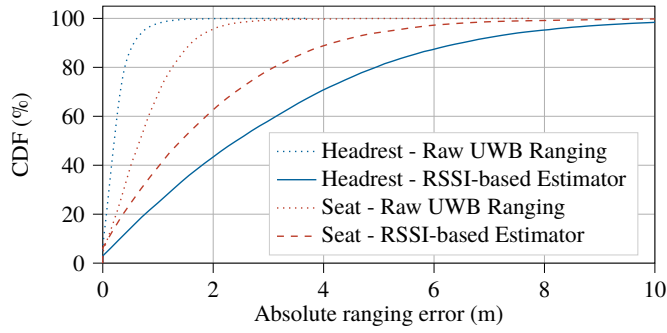


Fig. 6: Ranging error of an RSSI-based distance estimator

A value close to 0 indicates a strong single path in the CIR data, while a value close to 1 indicates multiple peaks with similar energy levels. This is illustrated in Figure 4, where the CIR measured indoor would have a value close to 0 due to its strong peak, while the one measured in the cabin would have a larger value, closer to 1 due to the presence of multipaths.

Results with respect to the ranging distance are presented in Figure 7. As expected, there is a strong correlation between the ranging distance and the multipath metric in the aircraft cabin. In the outdoor and indoor environments, the multipath metric remains close to constant.

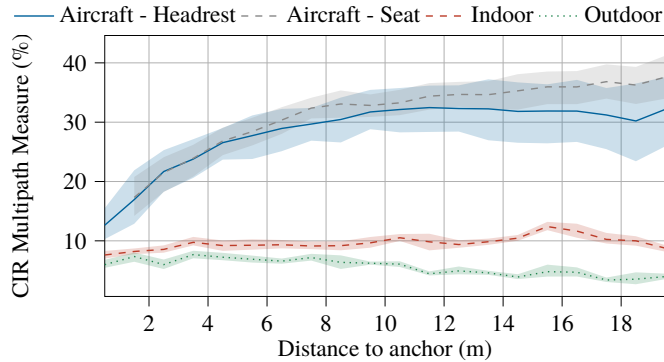


Fig. 7: Impact of distance between anchor and tag on multipath metric. Areas correspond to the 25 % and 75 % percentiles.

C. Ranging accuracy

We evaluate in this section the ranging accuracy, i.e. the accuracy of the individual distance measurements between tag and anchors. We use the absolute difference between measured and true range as our metric:

$$\text{ranging error} = |\text{range} - \text{range}_{\text{true}}| \quad (6)$$

Table II provides a summary of the impact of the different correction methods on the absolute ranging error. In the outdoor environment, we achieve decimeter level accuracy with the offset and LR corrections, with an average of 4 cm. In the aircraft environment, we notice a larger ranging error of 30 cm in average even after offset and LR correction. This

is especially visible at the tail of the statistical distribution as shown by the 95 % quantile.

The NN-based error correction brings a large benefit, almost matching the accuracy measured in the outdoor environment. Despite larger errors, the variant of the NN only using the input of one anchor (labeled NN 1A in Table II) still brings a benefit compared with the LR correction.

TABLE II: Summary of the absolute ranging error before and after correction methods

Env.	Method	Mean	Median	Q-95 %
Outdoor	Raw data	0.389 m	0.430 m	0.499 m
	Corr. w/ Offset	0.077 m	0.045 m	0.275 m
	Corr. w/ LR	0.040 m	0.033 m	0.103 m
Aircraft	RSSI estimator	2.520 m	1.944 m	6.835 m
	Raw data	0.604 m	0.411 m	1.728 m
	Corr. w/ Offset	0.335 m	0.223 m	0.968 m
	Corr. w/ LR	0.307 m	0.211 m	0.892 m
	NN 1A	0.160 m	0.113 m	0.486 m
	NN range pred.	0.044 m	0.020 m	0.169 m

D. Localization accuracy

We evaluate in this section the localization accuracy, i.e. the accuracy of the computed 2D coordinates based on the ranging measurements. We use the Euclidean distance to the true coordinates as our metric:

$$\text{localization error} = \sqrt{(x_T - x_{\text{true}})^2 + (y_T - y_{\text{true}})^2} \quad (7)$$

with (x_T, y_T) the computed coordinates of the tag after multilateration or the predicted coordinates from the NN.

Table III provides a summary of the impact of the corrections methods on the localization error. As for the previous results, larger ranging errors also lead to larger localization errors when the tag is placed on the seat compared with when it is placed on the headrest.

TABLE III: Summary of localization accuracy in the cabin

Method	Tag on seat		Tag on headrest	
	Mean	Q-90 %	Mean	Q-90 %
Raw data	0.923 m	1.883 m	0.354 m	0.871 m
Corrected w/ LR	0.379 m	0.639 m	0.199 m	0.418 m
NN range pred.	0.208 m	0.447 m	0.161 m	0.332 m
NN coord. pred.	0.167 m	0.268 m	0.142 m	0.288 m

Regarding the NN variants, the NN directly predicting the coordinates appears to result in a better accuracy compared with the NN predicting only ranges. This is explained by the additional multilateration process required for the range variant, since small errors on the ranging can propagate in the multilateration computation, leading to larger errors.

E. Seat assignment

Finally, we evaluate in this section the use-case where the tag has to be assigned to a seat based on its localization. This

is performed by assigning it to the closest known seat position given the computed coordinates. This is formalized as:

$$\underset{seat}{assigned} = \arg \min_{seat} \sqrt{(x_T - x_{seat})^2 + (y_T - y_{seat})^2} \quad (8)$$

with (x_{seat}, y_{seat}) the known locations of the different seats.

According to the cabin geometry presented in Figure 3, a seat assignment accuracy of 100 % would require a localization system with a maximum error of 0.226 m.

Accuracy results of the different methods are presented in Table IV. Since seat labels represent 2D coordinates (eg. seat 5A implies row 5 and column A), we split the accuracy in Table IV according to the x axis (i.e. seat row axis) and the y axis (i.e. seat letter axis) illustrated in Figure 3.

For most methods, we notice a large difference between the two axes, where the accuracy along the x axis is better than on the y axis. This is explained by the geometry of the aircraft cabin and the anchor placements within the cabin, making it more sensitive to small errors along the y axis.

TABLE IV: Seat assignment accuracy of the different methods

Tag Pos.	Method	Seat Accuracy	x Axis Accuracy	y Axis Accuracy
Headrest	Raw data	52.0 %	99.1 %	52.6 %
	Corrected w/ LR	74.8 %	99.7 %	75.1 %
	NN range pred.	83.8 %	100.0 %	83.8 %
	NN coord. pred.	87.5 %	100.0 %	87.5 %
	NN direct pred.	97.2 %	99.7 %	99.1 %
Seat	Raw data	18.6 %	60.2 %	36.6 %
	Corrected w/ LR	60.9 %	100.0 %	64.6 %
	NN range pred.	75.2 %	100.0 %	77.6 %
	NN coord pred.	91.9 %	99.4 %	96.9 %
	NN direct pred.	98.8 %	100.0 %	98.8 %

The results from Table IV match the ones from Section V-D and the requirement of 0.226 m. As previously, the NN directly predicting the seat label also achieves the best results, with an accuracy better than 97 %. This illustrates the impact of an end-to-end approach for training a NN.

VI. CONCLUSION

We presented in this work an Ultra-Wideband (UWB) based localization system targeting use-cases in aircraft cabins. Our main contribution is a measurement campaign performed in a real cabin of an Airbus A321 aircraft, as well as various methods for correcting ranging errors. Our measurements results confirm our previous findings from [5]. While our previous measurements were performed in a mockup of a small cabin section, the results presented here illustrate that UWB is indeed a valid candidate for an onboard aircraft localization system. With our end-to-end neural network (NN) approach, we were able to localize a tag with an average localization error of about 16 cm and assign it to a seat with an accuracy of 97 %. We also show that compared against a simpler system using only received signal strength indication (RSSI) – such as Bluetooth-based localization systems – UWB results in more accurate localization. Our measurements also confirm that an

aircraft cabin is a challenging environment for localization, due to the presence of many obstacles and propensity for multipath effects. Overall, we demonstrate the viability of the UWB technology for localization for the aircraft industry.

REFERENCES

- [1] A. Yassin, Y. Nasser, M. Awad, A. Al-Dubai, R. Liu, C. Yuen, R. Raulefs, and E. Aboutanios, "Recent advances in indoor localization: A survey on theoretical approaches and applications," *IEEE Commun. Surveys Tuts.*, 2017.
- [2] F. Zafari, A. Gkelias, and K. K. Leung, "A survey of indoor localization systems and technologies," *IEEE Commun. Surveys Tuts.*, 2019.
- [3] S. Chiu, J. Chuang, and D. G. Michelson, "Characterization of UWB channel impulse responses within the passenger cabin of a Boeing 737-200 aircraft," *IEEE Trans. Antennas Propag.*, 2010.
- [4] S. Chiu and D. G. Michelson, "Effect of human presence on UWB radiowave propagation within the passenger cabin of a midsize airliner," *IEEE Trans. Antennas Propag.*, 2010.
- [5] C. G. Karadeniz, F. Geyer, T. Multerer, and D. Schupke, "Precise UWB-Based Localization for Aircraft Sensor Nodes," in *Proc. of the IEEE/AIAA 39th Digital Avionics Systems Conference*, 2020.
- [6] J. F. Schmidt, D. Neuhold, C. Bettstetter, J. Klaue, and D. Schupke, "Wireless connectivity in airplanes: Challenges and the case for UWB," *IEEE Access*, 2021.
- [7] T. Multerer, F. Geyer, S. Duhovnikov, A. Baltaci, J. Tepper, and D. Schupke, "A Localizable Wireless Communication Node with Remote Powering for Onboard Operations," in *Proc. of the IEEE/AIAA 40th Digital Avionics Systems Conference*, ser. DASC 2021, 2021.
- [8] Z. Irahauten, H. Nikoosar, and G. Janssen, "An overview of ultra wide band indoor channel measurements and modeling," *IEEE Microw. Wireless Compon. Lett.*, 2004.
- [9] T. Ye, M. Walsh, P. Haigh, J. Barton, and B. O'Flynn, "Experimental impulse radio IEEE 802.15.4a UWB based wireless sensor localization technology: Characterization, reliability and ranging," in *Proc. of the 22nd IET Irish Signals and Systems Conference*, 2011.
- [10] Q.-T. Ngo, P. Roussel, B. Denby, and G. Dreyfus, "Correcting non-line-of-sight path length estimation for ultra-wideband indoor localization," in *Proc. of the 2015 Int. Conf. on Localization and GNSS*, 2015.
- [11] F. Bandiera, A. Coluccia, and G. Ricci, "A cognitive algorithm for received signal strength based localization," *IEEE Trans. Signal Process.*, 2015.
- [12] G. Schroeder, "A real-time UWB multi-channel indoor positioning system for industrial scenarios," in *2018 International Conference on Indoor Positioning and Indoor Navigation (IPIN)*, 2018.
- [13] A. Ledergerber, M. Hamer, and R. D'Andrea, "Angle of arrival estimation based on channel impulse response measurements," in *Proc. of the 2019 IEEE/RSJ Int. Conf. on Intelligent Robots and Systems*, 2019.
- [14] A. Ledergerber and R. D'Andrea, "A multi-static radar network with ultra-wideband radio-equipped devices," *Sensors*, 2020.
- [15] S. Kram, M. Stahlke, T. Feigl, J. Seitz, and J. Thielecke, "UWB channel impulse responses for positioning in complex environments: A detailed feature analysis," *Sensors*, 2019.
- [16] J. B. Andersen, K. L. Chee, M. Jacob, G. F. Pedersen, and T. Kurner, "Reverberation and absorption in an aircraft cabin with the impact of passengers," *IEEE Trans. Antennas Propag.*, 2012.
- [17] D. Neuhold, J. F. Schmidt, J. Klaue, D. Schupke, and C. Bettstetter, "Experimental study of packet loss in a UWB sensor network for aircraft," in *Proc. of the 20th ACM Int. Conf. on Modelling, Analysis and Simulation of Wireless and Mobile Systems*, 2017.
- [18] H. Bai, M. Atiquzzaman, and D. Lilja, "Wireless sensor network for aircraft health monitoring," in *First International Conference on Broadband Networks*, 2004.
- [19] R. K. Yedavalli and R. K. Belapurkar, "Application of wireless sensor networks to aircraft control and health management systems," 2011.
- [20] M. Losada, A. Irizar, P. del Campo, P. Ruiz, and A. Leventis, "Design principles and challenges for an autonomous WSN for structural health monitoring in aircrafts," in *Design of Circuits and Integrated Systems*, 2014.
- [21] Decawave, "The effect of channel characteristics on time-stamp accuracy in DW1000 based systems," Tech. Rep. APS006, 2014, version 1.03.